BER Performance Evaluation for CPFSK Phase and Polarization Diversity Coherent Optical Receivers

Jerzy Siuzdak and W. van Etten, *Senior Member, IEEE*

***Abstract*—The following methods of CPFSK signals demodulation are compared for phase and polarization diversity receivers: single filter, dual filter, delay and multiply. BER values are obtained in each case showing that for negligible laser linewidths the delay demodulation method outperforms the dual-filter method by approximately 3 dB, and the single-filter method by 6 dB. Since the noise bandwidth for MSK and delay demodulation is approximately twice as small as for the other methods, one should add another 3 dB to get the gain for that modulation/demodulation method. The influences of nonzero laser linewidth, noise correlation, and non-Gaussian character of the probability density functions of the noise at the sampler have been taken into account.**

I. Introduction

CONTINUOUS phase frequency shift keying (CPFSK) is potentially a promising technique for coherent optical signal modulation, since direct modulation of the laser current may be employed and the insertion loss of an external modulator is avoided [1]–[3]. The performance of such a system using heterodyne demodulation has been investigated in numerous papers [3]–[8]. There is, however, another approach to the demodulation which uses a multiport optical network that provides a means for recovering the amplitude and phase of the optical signal. It does not require phase locking of optical sources and converts an incoming signal directly to baseband. This is called phase diversity and is often combined with the independent reception of orthogonally polarized components of the optical signal (the so-called polarization diversity). Polarization diversity involves decomposition of the input light into two orthogonal polarization states, independent detection of the signals in these states and subsequent electronic processing. A lot of work has been devoted to the investigation of ASK and DPSK systems employing phase (and polarization) diversity [9]–[12]. Less is known, however, about CPFSK phase (and polarization) diversity schemes, especially about schemes that employ the delay-and-multiply demodulation technique [13]. The topics that will be addressed here are dealt with in [20] and [21], but the analysis of [20] does not include the lasers' phase noise, whereas [21] does not account for the non-Gaussian character of the probability density functions of the noise at the sampler. Moreover, both papers neglect the noise correlation. In this paper, we shall calculate bit error rates for various phase and polarization diversity demodulation schemes of CPFSK signals. To this end, we shall use actual non-Gaussian probability density functions (pdf's) of signals at the input of a threshold comparator, since the Gaussian approximation often leads to inaccurate results [7]. We shall also investigate the impact of the laser phase noise and receiver noise correlation on the performance of these receivers. In this paper we study two types of receivers:

1) phase diversity receivers in which the polarization states of the received and local oscillator signals are matched by means of some polarization control scheme, and
2) phase and polarization diversity receivers.

Our analysis is done under the assumption that the shot noise related to the local oscillator laser dominates other noise sources (such as the thermal noise). We assume that intersymbol interference is absent. The local oscillator intensity noise is not included in the analysis. There are receiver structures that suppress this kind of noise. For the sake of clarity some mathematical derivations are placed in appendixes.

II. Receivers Preliminary

A phase-diversity receiver is shown schematically in Fig. 1. It consists of a $\{2 \times 2\}$ or $\{3 \times 3\}$ optical network, photodetectors, and a demodulation scheme to be described later. The $\{2 \times 2\}$ optical network is assumed to be a 90° optical hybrid [14], [15], which is not a standard $\{2 \times 2\}$ optical directional coupler. A polarization diversity receiver is shown in Fig. 2. It consists of two polarization beamsplitters, two phase-diversity receivers of either type, a summing circuit, and a threshold comparator. Both the signal and local oscillator (LO) light are fed to polarization splitting couplers, which produce orthogonal polarization components of the incoming light which are inputs to the two phase-diversity receivers. The polarization plane of linearly polarized LO light is chosen so that its power is equally divided between two orthog-

Manuscript received January 10, 1991; revised May 27, 1991. J. Siuzdak was supported in part by Nederlandse Organisatie voor Wetenschappelijk Onderzoek (NWO).

J. Siuzdak is with the Faculty of Electrical Engineering, Eindhoven University of Technology, 5600 MB Eindhoven, The Netherlands, on leave from the Instytut Telekomunikacji PW, Warsaw, Poland.

W. van Etten is with the Faculty of Electrical Engineering, Eindhoven University of Technology, 5600 MB Eindhoven, The Netherlands.

IEEE Log Number 9102964.

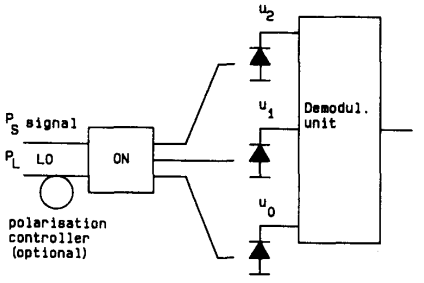

Fig. 1. Phase diversity optical receiver: ON—{2 × 2} or {3 × 3} optical network.

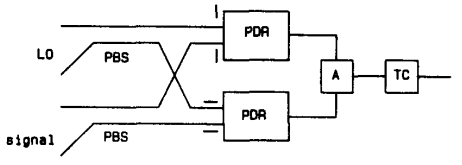

Fig. 2. Polarization diversity receiver: PBS—polarization beamsplitter, PDR—phase diversity receiver, A—adder, TC—threshold comparator.

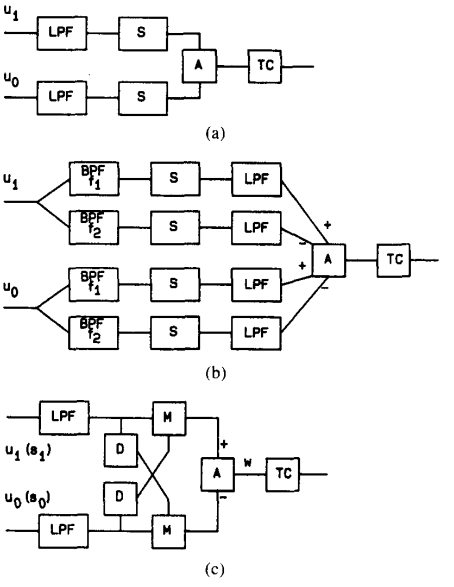

Fig. 3. Different methods of demodulation of CPFSK signals: A) single filter, B) dual filter, C) delay and multiply. LPF—low-pass filter, S—squarer, A—adder, TC—threshold comparator, BPF—bandpass filter, D—delay line, M—multiplier. In the case of the {3 × 3} receiver, there is a third branch not marked in figs. A, B, and quadrature signals s_0, s_1 are obtained from u_k.

onal polarization states. The outputs of the two multiport receivers are then added.

In the sequel, we treat in detail only the phase diversity receivers because, as we shall see, the extension of the results for phase and polarization diversity receivers is straightforward.

The signals at the outputs of the photodetectors of either phase-diversity receiver are [9], [16]

$$u_k = R\sqrt{P_s P_l}\cos\left[\alpha(t) + \theta(t) + k\pi/2\right], \quad k = 0, 1, \tag{1}$$

$$u_k = (2/3)R\sqrt{P_s P_l}\cos\left[\alpha(t) + \theta(t) + k(2/3)\pi\right], \quad k = 0, 1, 2. \tag{2}$$

Equation (1) holds for the {2 × 2} and (2) for the {3 × 3} receiver. In the equations above, R is the responsivity of the photodetectors, P_s is the power of the received signal, P_l denotes the power of the local oscillator, $\theta(t)$ is the lasers phase noise, and

$$\alpha(t) = 2\pi f_0 t + (\pi h/T)\int_{-\infty}^{t}\sum_k b_k \operatorname{rect}(\tau - kT)\,d\tau. \tag{3}$$

Here f_0 is the frequency offset between the lasers, h is the modulation index and $\{b_k\}$ is the symbol sequence, taking on the values -1 or $+1$. The function rect (t) is equal to 1 if $t \in (0, T)$ and 0 elsewhere. Here T is the bit duration. The modulation index $h = (f_1 - f_2)T$, where f_1 and f_2 are the frequencies corresponding to "-1" and "$+1$" symbols, respectively.

The shot-noise terms at the outputs of the photodetectors are independent and it is reasonable to assume them to be white and Gaussian. They have the power spectral densities

$$N_2 = qRP_l/2 \tag{4}$$

$$N_3 = qRP_l/3 \tag{5}$$

when it is assumed $P_l >> P_s$. Here N_2 corresponds to the {2 × 2} receiver and N_3 to the {3 × 3} receiver. At this stage, it is easy to incorporate the thermal noise into the analysis, just by adding thermal noise terms to the power spectral densities. It will not be done here because the shot noise will dominate in a properly designed scheme.

Let us examine various demodulation schemes depicted in Fig. 3. Each of the receivers comprises a low-pass or band-pass filter to which the signals from the photodetectors are fed. In the single filter demodulator (Fig. 3(a)), during the transmission of one of the symbols ("-1" for example) the frequencies of both the lasers are set equal, which corresponds to shifting the spectrum to baseband. The modulation index is chosen large enough to sweep all the frequency components out of the baseband while transmitting the symbol "$+1$." Thus the signal is present at the output of each low-pass filter of this scheme only when a "-1" is transmitted. This is in fact equivalent to the ASK demodulation scheme described elsewhere [9].

In the dual-detector scheme of Fig. 3(b), the modulation index is again chosen large enough to avoid overlapping of the spectra corresponding to the "-1" and "$+1$" symbols. There are two band-pass filters for each branch,

each of them tuned to the frequency of the corresponding symbol. Then the outputs of the filters are squared and appropriately combined and a decision device selects the greater output.

In the delay demodulation scheme of Fig. 3(c), the frequency offset between the lasers is zero, so the symbols "-1" and "$+1$" occupy the same baseband spectrum. They may be distinguished only after employing the delay and multiply technique [13].

The filters in the demodulation schemes are chosen to be ideal rectangular filters with equivalent baseband transfer function $H(f) = 1$ for $-B/2 < f < B/2$ and 0 elsewhere. Furthermore, it is assumed that the bandwidth of these filters is broad enough, so that they do not influence the form of the information signal. The filtered shot noise power is proportional to B. The value of B is selected to pass 95% of the information signal power. This is a somewhat artificial assumption, nevertheless it is often used [8] and leads to a reasonable receiver bandwidth.

III. Bandwidth Requirements

Each of the signals u_k given by (1), (2) may be represented in the form

$$u_k = \text{Re}\ \{u(t) \exp\ [2\pi f_0 t + \theta(t)]\} \tag{6}$$

where $u(t)$ is the equivalent baseband information-bearing signal, and the other factor corresponds to the unmodulated laser signal. It follows from the above that the equivalent low-pass signal spectrum $\Phi(f)$ is the convolution of the lasers spectrum $L(f)$ with the spectrum of the signal $u(t)$ denoted by $\Phi_u(f)$

$$\Phi(f) = \int_{-\infty}^{\infty} \Phi_u(x) L(f - x)\, dx. \tag{7}$$

The low-pass equivalent of the Lorentzian spectrum is given by

$$L(f) = \frac{2}{\pi\delta_1 \left\{1 + \dfrac{4f^2}{(\delta_1)^2}\right\}} \tag{8}$$

where δ_1 is the sum of the (FWHM) transmitter and LO lasers linewidths, and unit power was assumed. Thus the power within the band $(-B/2, B/2)$ is given by

$$\begin{aligned} P_b &= \int_{-B/2}^{B/2} \Phi(f)\, df \\ &= \frac{1}{\pi} \int_{-\infty}^{\infty} \Phi_u(f) \left\{ \text{arctg} \left[\left(\frac{BT}{2} - f \right) \Big/ \epsilon \right] \right. \\ &\quad \left. + \text{arctg} \left[\left(\frac{BT}{2} + f \right) \Big/ \epsilon \right] \right\} df. \end{aligned} \tag{9}$$

Here $\epsilon = \delta_1 T/2$. We have used (7), (8), normalized the frequency to the bit rate and interchanged the order of integration. Unfortunately, the form of $\Phi_u(f)$ [17] (given in Appendix 1) is rather complicated, so numerical integration was necessary. In Fig. 4, the results are presented for a baseband filter, i.e., for a zero frequency offset between the lasers. In the case of a bandpass filter, the filter passband width is twice as large. We can readily see that the bandwidth of the filter increases almost linearly with the increase of the modulation index h and depends rather slightly on $\delta_1 T$ for the given values of this parameter. Such a dependence is consistent with Carson's rule.

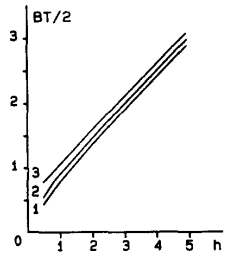

Fig. 4. Normalized 95% low-pass filter bandwidth $BT/2$ versus the modulation index h: 1) $\delta_1 T = 0$, 2) $\delta_1 T = 5\%$, 3) $\delta_1 T = 10\%$.

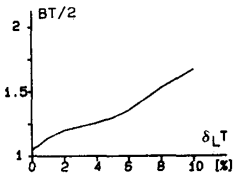

Fig. 5. Normalized 95% low-pass filter bandwidth $BT/2$ for $h \gg 1$ against $\delta_1 T$.

For large modulation indices $h \gg 1$, which are necessary to avoid overlapping of the spectra of two modulating frequencies when single or double filter demodulation is used, the equivalent low-pass spectrum is proportional to (Appendix A)

$$\Phi_u(f) \sim \left[\frac{\sin\ (\pi f)}{\pi f} \right]^2 [1 + \cos\ (2\pi f)]. \tag{10}$$

The bandwidth of the low-pass filter that passes 95% of the signal power for the spectrum as above, is given in Fig. 5. Again, the bandwidth of the bandpass filter is twice as large.

For the near zero laser linewidths the equivalent noise bandwidths follow from Figs. 4 and 5, respectively,

$$B \approx 1/T \quad \text{for } h \approx 0.5 \tag{11}$$

$$B \approx 2/T \quad \text{for } h \gg 1. \tag{12}$$

IV. Dual-Filter Demodulation

As we have mentioned before, for the same peak powers (i.e., for the mean power twice as large), the performance of the single-filter demodulation scheme is fully equivalent to that of the ASK demodulation scheme de-

scribed elsewhere [9], and those results may be applied directly with an appropriate substitution of the noise bandwidth. Thus this scheme will not be considered here and the reader is referred to [9]. We shall present only the final results.

In the case of the dual-filter scheme let us assume that both filters have the same pass bandwidths in each branch. Thus, using (4) with the factor 2 (which follows from bandpass filtering) taken into account, we get for the noise powers at the inputs of the squaring devices

$$\langle n_k^2 \rangle = qRP_1B \qquad k = 0, 1 \tag{13}$$

$$\langle n_k^2 \rangle = 2qRP_1B/3 \qquad k = 0, 1, 2. \tag{14}$$

Equation (13) holds for the $\{2 \times 2\}$ receiver and (14) for the $\{3 \times 3\}$ receiver. Let us consider the $\{2 \times 2\}$ receiver for example and the output of the filter tuned to the frequency f_1 in the 0-th branch. When the symbol corresponding to this frequency is actually transmitted, then this output reads as follows:

$$R\sqrt{P_1P_s}\cos[\alpha(t)] + n_{0c}(t)\cos[\alpha(t)] + n_{0s}(t)\sin[\alpha(t)] \tag{15}$$

where $n_{0c}(t)$ and $n_{0s}(t)$ are the quadrature components of the noise $n_0(t)$; they are independent and have the same powers as $n_0(t)$. After squaring and rejecting the double frequency terms by the low-pass filters that follow the squaring devices, we get at the input of the summing circuit

$$(\sqrt{2\text{SNR}} + n_c)^2 + n_s^2. \tag{16}$$

Here we have normalized the noises to unit variances and defined the signal to noise ratio SNR as

$$\text{SNR} = RP_s/(qB). \tag{17}$$

The output of the filter tuned to the other frequency (f_2) is then

$$n_c'^2 + n_s'^2 \tag{18}$$

where these noises are independent and have unit variances. After adding the contribution of the other branch of the receiver we readily see that the pdf of the square root of the signal is the generalized chi pdf of the fourth order (four degrees of freedom, $N = 4$) [9] and with the noncentral parameter A^2 equal to 2SNR. The general form of this distribution is given by

$$p_\chi(\chi) = \chi^{N/2}\text{I}_{N/2-1}(A\chi)\exp[-(\chi^2 + A^2)/2]/A^{N/2-1}, \qquad \chi > 0 \tag{19}$$

where I represents the modified Bessel function of the first kind.

On the other hand, the pdf of the square root of the noise alone is chi with $N = 4$ degrees of freedom [9] and is given by

$$p_\xi(\xi) = 2/[2^{N/2}\Gamma(N/2)]\xi^{N-1}\exp(-\xi^2/2), \qquad \xi > 0 \tag{20}$$

where Γ is the gamma function.

It is easy to show for other kinds of receivers that the form of the probability distribution functions is also represented by (19) and (20) with the noncentral parameter unchanged, and with an appropriate change of N

$N = 6$ for the $\{3 \times 3\}$ phase-diversity receiver,

$N = 8$ for the $\{2 \times 2\}$ phase and polarization diversity receiver, and

$N = 12$ for the $\{3 \times 3\}$ phase and polarization diversity receiver.

Since we have assumed no frequency overlap, the variables χ and ξ are independent. As the sign of $\chi - \xi$ determines the decision of the threshold comparator, it chooses the wrong possibility if $\xi > \chi$. When the two symbols are equally probable we have due to the symmetry

$$\text{BER} = \int_0^\infty p_\chi(\chi)\,d\chi \int_\chi^\infty p_\xi(\xi)\,d\xi. \tag{21}$$

Such integrals have been calculated in [9]. Here we present two results only

$$\text{BER} = 0.5\exp(-\text{SNR})(1 + \text{SNR}/4) \tag{22}$$

for the $\{2 \times 2\}$ phase-diversity receiver, and

$$\text{BER} = 0.5\exp(-\text{SNR})(1 + 3\text{SNR}/8 + \text{SNR}^2/32) \tag{23}$$

for the $\{3 \times 3\}$ phase-diversity receiver.

At this point two remarks have to be made.

1) Note that in this case the noise in each arm of the receiver consists of a bandpass process, which can be represented by two independent quadrature components (n_s and n_c). This is contrary to our former paper [9], where the noise terms were lowpass, and it means that there are twice as many independent noise terms as arms in the receiver. That is why the performance of the present $\{3 \times 3\}$ phase-diversity receiver is equivalent to the performance of the former [9] $\{3 \times 3\}$ phase and polarization receiver.

2) In our former paper [9] the third term of (23) was in error; now (23) is correctly presented here.

The results are shown in Fig. 6 where they are compared with the single-filter method. One can readily see that the dual-filter demodulation requires an SNR which is roughly 3 dB less in order to achieve the same performance as the single-filter method. It should be stressed however, that from an SNR point of view, the phase-diversity technique is of little advantage in the dual detection scheme as the common heterodyning technique without phase diversity leads to similar sensitivities with a simpler implementation. Anyway, phase diversity relaxes the h.f. requirements of the i.f. filters and processing electronics. The differences between the results here and those in [9] are caused by different low-pass filters in the demodulation circuits.

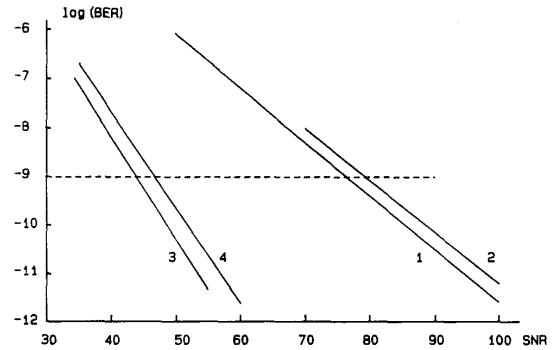

Fig. 6. Comparison of the BER for single- and dual-filters demodulation methods. Single filter: 1) {2 × 2} phase-diversity receiver, 2) {3 × 3} phase-diversity receiver. Dual filter: 3) {2 × 2} phase-diversity receiver, 4) {3 × 3} phase-diversity receiver.

Another method of detection appears attractive at first glance: combining the dual- and single-filter methods by shifting one of the filters to the baseband in the dual-filter method. In this case however, the threshold is nonzero as the receiver is no longer symmetric; it should be optimized according to the signal and noise statistics and this is a main practical disadvantage. In addition, it does not offer a substantial BER improvement. To prove this let us note that, for the {2 × 2} phase-diversity receiver for example, the statistics of the signal channel is the generalized chi with $N = 2$ (baseband) or $N = 4$ (passband) depending on which symbol is sent, whereas the statistics of the noise channel is chi with $N = 2$ or $N = 4$, accordingly.

V. Delay Demodulation

For this demodulation f_0 should be zero. Furthermore, in order to achieve maximum sensitivity, the values of the delay τ and the modulation index h have to satisfy [4], [7]

$$h = T/(2\tau). \tag{24}$$

This ensures the quadrature relation between the delayed signals.

A. The {2 × 2} Receiver

Let us begin with the {2 × 2} phase-diversity receiver. When the condition (24) is met the values of the signals after delay are

$$u_k(t - \tau) = R\sqrt{P_s P_l}\cos[\alpha(t) + \theta(t - \tau) \pm \pi/2 + k\pi/2], \quad k = 0, 1 \tag{25}$$

where the sign "+" or "−" depends on which symbol was transmitted. Let us consider the "−" sign for example, as the other case is dual. The signal after multiplication and subtraction is at the moment of sampling, t_s

$$\begin{aligned} w &= [u_1(t_s) + n_1(t_s)][u_0(t_s - \tau) + n_0(t_s - \tau)] \\ &\quad - [u_0(t_s) + n_0(t_s)][u_1(t_s - \tau) + n_1(t_s - \tau)] = \\ &= A^2\cos\Delta + n_1 A\sin(\alpha + \Delta) + n_0' A\sin\alpha \\ &\quad + n_0 A\cos(\alpha + \Delta) - n_1' A\cos\alpha + n_1 n_0' - n_1' n_0. \end{aligned} \tag{26}$$

Here

$$\alpha = \alpha(t_s) + \theta(t_s) \tag{27}$$

$$\Delta = \theta(t_s - \tau) - \theta(t_s) \tag{28}$$

and $'$ denotes the delayed version of the corresponding noise terms at the moment of sampling. To simplify the analysis let us normalize (26) to obtain unit noise variances. This does not change the BER values since the threshold is zero. In this case

$$A^2 = 2\text{SNR}. \tag{29}$$

Note however, that in this case the bandwidth B may be substantially smaller than in the case of the dual-filter detection as lower values of h may be used (see (11) and (12), and Figs. 4 and 5). Furthermore, we have

$$\langle n_0 n_1\rangle = \langle n_0 n_1'\rangle = \langle n_0' n_1\rangle = \langle n_0' n_1'\rangle = 0 \tag{30}$$

as the noise terms n_0 and n_1 are independent and

$$\langle n_0 n_0'\rangle = \langle n_1 n_1'\rangle = \rho \tag{31}$$

where ρ is the noise correlation coefficient given by

$$\rho = \rho(\tau) = \sin(y)/y \tag{32}$$

with

$$y = \pi BT/(2h) \tag{33}$$

and B is the 95% bandwidth. Deriving the above we used (24).

The error probability in detecting a bit with the "−" sign, which is equal to the BER due to symmetry in this case, is the probability that $w < 0$. It is shown in Appendix B that this probability for a given Δ may be expressed by (21) where the functions $p_\chi(\chi)$ and $p_\xi(\xi)$ are the pdf's of the generalized chi distribution of $N = 2$

$$p_x(x) = x\exp[-(x^2 + A_x^2)/2]\mathrm{I}_0(A_x x) \tag{34}$$

and noncentral parameters

$$A_\chi^2 = \frac{2\text{SNR}[1 + \sqrt{1 - \rho^2}\cos\Delta - \rho\sin\Delta]}{1 - \rho^2} \tag{35}$$

$$A_\xi^2 = \frac{2\text{SNR}[1 - \sqrt{1 - \rho^2}\cos\Delta - \rho\sin\Delta]}{1 - \rho^2}. \tag{36}$$

Based on the results in Appendix B, it is straightforward to show that for the {2 × 2} phase and polarization diversity receiver the BER is also given by (21) with the functions $p_\chi(\chi)$ and $p_\xi(\xi)$ being pdf's of the generalized

chi distribution of $N = 4$ and identical noncentral parameters given by (35) and (36), respectively.

Equation (21) together with (35) and (36) give the value of BER (Δ) for a particular realization of the phase-noise process Δ. To obtain the value of BER of an actual receiver it is necessary to average BER (Δ) over all realization of Δ. It is usually assumed [11], [18] that Δ has the Gaussian pdf with zero mean and variance

$$\sigma^2 = 2\pi\delta_1\tau \tag{37}$$

i.e.,

$$p_\Delta(\Delta) = \frac{\exp\left[-\Delta^2/(2\sigma^2)\right]}{\sqrt{2\pi}\,\sigma}. \tag{38}$$

Thus we have finally

$$\text{BER} = \int_{-\infty}^{\infty} p_\Delta(\Delta)\,d\Delta \int_0^{\infty} p_\chi(\chi)\,d\chi \int_\chi^{\infty} p_\xi(\xi)\,d\xi. \tag{39}$$

The values of the BER are calculated numerically for both the receivers and the results shown in Fig. 7, whereas Fig. 8 shows the excess of power necessary to obtain BER $= 10^{-9}$ against the value of $\delta_1\tau$ for various ρ. The following conclusion may be drawn from the calculations:

1. Both the $\{2 \times 2\}$ phase and $\{2 \times 2\}$ phase and polarization diversity receivers perform very similarly especially for greater laser linewidths.

2. The noise correlation cancels to some extent the influence of the nonzero laser linewidths, but it does not shift the BER floor.

In the absence of the noise correlation and for zero laser linewidths, the expressions for the BER can be obtained in a closed form [9]

$$\text{BER} = 0.5\exp(-\text{SNR}) \tag{40}$$

$$\text{BER} = 0.5\exp(-\text{SNR})(1 + \text{SNR}/4). \tag{41}$$

Equation (40) holds for the $\{2 \times 2\}$ phase-diversity receiver, whereas (41)—for the $\{2 \times 2\}$ phase and polarization diversity receiver. This confirms the well established fact [1] that DPSK receivers and CPFSK receivers that employ the delay and multiply technique, have the same performance.

In the absence of the noise correlation yet for nonnegligible laser linewidth our analysis gives identical results as are obtained in [1], [11], [18]. On the other hand, our results differ from those obtained in [7] for nonzero noise correlation, since the noise correlation was obtained there by violating a condition similar to (24).

B. The $\{3 \times 3\}$ Receiver

In order to apply the delay demodulation scheme, the quadrature signals s_0 and s_1 should be obtained by an appropriate combination of three signals u_k given by (2) and which are shifted by 120°. Here are a few possibilities

$$s_0 = 2u_0 - u_1 - u_2, \qquad s_1 = u_1 - u_2, \tag{42}$$

$$s_0 = u_0 - u_1 - u_2, \qquad s_1 = u_1 - u_2, \tag{43}$$

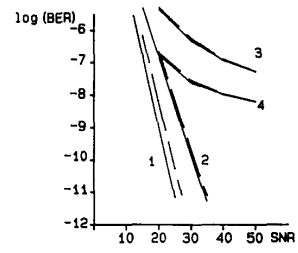

Fig. 7. BER for $\{2 \times 2\}$ phase-diversity receiver (solid lines), and for $\{2 \times 2\}$ phase and polarization diversity receiver (dashed lines) with the delay demodulation. $\delta_1\tau = 0$: 1) $\rho = 0$, 2) $\rho = 0.5$. $\delta_1\tau = 1\%$: 3) $\rho = 0$, 4) $\rho = 0.5$.

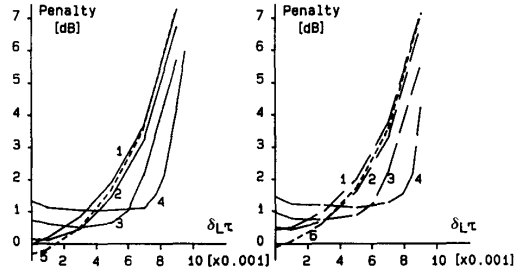

Fig. 8. Delay demodulation. Signal power excess, as compared with SNR = 20, necessary to obtain BER $= 10^{-9}$ against $\delta_1\tau$ with ρ as a parameter. Solid lines $\{2 \times 2\}$—phase diversity receiver, dashed lines—$\{2 \times 2\}$ phase and polarization diversity receiver: 1) $\rho = 0$, 2) $\rho = 0.1$, 3) $\rho = 0.3$, 4) $\rho = 0.5$. Dotted lines—$\{3 \times 3\}$ receivers (the worst case): 5) phase-diversity receiver, 6) phase and polarization diversity receiver.

$$s_0 = s_0, \qquad s_1 = u_1 - u_2. \tag{44}$$

It is interesting to note that the method of (42) enables one to completely suppress the relative intensity noise (RIN), if any exists. We shall treat this case in greater detail, whereas only final results for the other two cases will be given as the analysis is similar then.

The quadrature signals and their delayed versions are in this case

$$s_0 = A\cos\alpha + (2n_0 - n_1 - n_2)/3,$$

$$s_1 = -A\sin\alpha + (n_1 - n_2)/\sqrt{3} \tag{45}$$

$$s_0' = -A\sin(\alpha + \Delta) + (2n_0' - n_1' - n_2')/3,$$

$$s_1' = -A\cos(\alpha + \Delta) + (n_1' - n_2')/\sqrt{3}. \tag{46}$$

Here $A^2 = (4/3)\text{SNR}$ as we have normalized the noise terms to unit variances. The signal at the input of the threshold comparator reads

$$w = s_1 s_0' - s_0 s_1'. \tag{47}$$

The error probability, which is equal to the BER due to symmetry in this case, is the probability that $w < 0$. It is shown in Appendix C that this probability for a given Δ and α may be expressed by (21), where the functions $p_\chi(\chi)$ and $p_\xi(\xi)$ are the pdf's of the generalized chi distribution

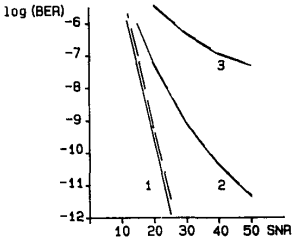

Fig. 9. Delay demodulation. BER values (the worst case) for $\{3 \times 3\}$ receivers. Solid lines—phase diversity receiver, dashed lines—phase and polarization diversity receiver: 1) $\delta_1 \tau = 0$, 2) $\delta_1 \tau = 0.5\%$, 3) $\delta_1 \tau = 1\%$.

of $N = 2$ given by (34) and noncentral parameters

$$A_\chi^2 = 2\text{SNR}\,\{1 + 0.25[\sin^2(\alpha + \Delta) + \cos^2\alpha] + \sqrt{1.5}\cos\Delta\} \quad (48)$$

$$A_\xi^2 = 2\text{SNR}\,\{1 + 0.25[\sin^2(\alpha + \Delta) + \cos^2\alpha] - \sqrt{1.5}\cos\Delta\}. \quad (49)$$

Based on the results in Appendix C, it is straightforward to show that for the $\{2 \times 2\}$ phase and polarization diversity receiver the BER value for a given α and Δ is also expressed by (21) with the functions $p_\chi(\chi)$ and $p_\xi(\xi)$ being pdf's of the generalized chi distribution of $N = 4$ and identical noncentral parameters given by (48) and (49).

Equation (21) together with (48) and (49) give the value of the BER (Δ, α) for a particular realization of the phase-noise process Δ and a given phase angle α. To obtain the value of BER in the worst case it is necessary to average BER (Δ, α) over all possible realization of Δ and then select that value of α for which the BER has a maximum. It is accomplished by means of (38) and (39).

The values of the BER are calculated numerically for both the $\{3 \times 3\}$ phase (and polarization) diversity receivers and shown in Fig. 9, whereas Fig. 8 shows again the excess of power necessary to obtain BER $= 10^{-9}$ against the value of $\delta_1 \tau$. It is readily seen from these figures that both receivers perform very similarly, especially for wider laser linewidths. Their performance is also very similar (slightly better for narrow laser linewidths) to that of the $\{2 \times 2\}$ receivers.

By asymptotic methods similar to that applied in [9] it is straightforward to show using (21), (48), and (49) that for zero laser linewidths the value of the BER for $\{3 \times 3\}$ receivers is proportional to $\exp(-\text{SNR})$.

In the same way as done for (42), the values of the BER may be obtained also for the other two methods of extracting quadrature signals given by (43) and (44). In these cases the BER is proportional to, respectively

$$\text{BER} \sim \exp(-8\text{SNR}/9)$$

$$\text{BER} \sim \exp(-2\text{SNR}/3)$$

i.e., the first method is superior. In the absence of laser phase noise, it gives roughly 3-dB gain as compared with the dual-filter demodulation method. For low modulation indexes $h \approx 0.5$, one should add to this gain another 3 dB as the equivalent low-pass filter bandwidth is twice as small as for the delay demodulation ((11) and (12)).

VI. Discussion

Based on the results of the previous paragraphs and those of [9] we are able to compare the various demodulation methods for negligible laser linewidths and zero noise correlation. This will be done on the basis of the values of the SNR necessary to obtain BER $= 10^{-9}$. The results are presented in Table I. Note however, that the value of the SNR is defined here as the signal to noise ratio at the output of the equivalent low-pass filter. Therefore, the SNR will be equivalent to the number of photons per bit received. The equivalent low-pass filter bandwidth requirements are the same for the single- and dual-filter demodulation methods, whereas they are not for the delay demodulation method as the bandwidth depends then on the modulation index h. It follows from spectral considerations that for low modulation indexes $h \approx 0.5$, this bandwidth is twice as small as for the other methods, so one should add another 3 dB to the gain of the delay demodulation method.

In this table the figures for the different ideal heterodyne receivers are related to those derived in [19], where the single-filter case is taken 3 dB worse than ASK and the delay method is taken to be equal to the PSK case, in accordance to (40) and (41). Let us consider the selection of the optimum demodulation method for a given value of $\delta_1 T$. In the single- and dual-filter demodulation method, a nonzero laser linewidth results only in a proportional increase of the 95% filter bandwidth according to Fig. 5. The situation is different for the delay demodulation. Here, the performance depends on the choice of the modulation index h. We shall consider the $\{2 \times 2\}$ phase-diversity receiver as the other receivers perform similarly. For a given $\delta_1 T$ and h, the value of τ may be easily obtained from (24) and there is a unique value of the 95% bandwidth which may be determined from (9). This in its turn gives via (32) and (33) the value of ρ. The above values are sufficient to determine the value of the BER from (39). The greater the h the greater the bandwidth B is and the greater the noise influence but the less the influence of the laser linewidth, on the other hand. This is a great advantage of CPFSK over DPSK that by increasing h we can handle substantial laser linewidths. It follows that for a given $\delta_1 T$ there is an optimum h which gives the smallest BER.

The calculations described above were actually performed and the results are shown in Fig. 10. The optimum value of h was found for each $\delta_1 T$ and the excess of power necessary to obtain a BER $= 10^{-9}$ (as compared with the delay demodulation with the filter given by (11)) is marked in this figure. The same values are depicted for the dual-filter demodulation method and heterodyne detection. It

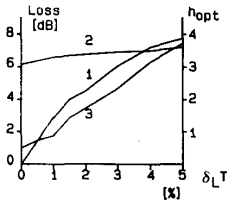

Fig. 10. The excess of power necessary to obtain BER = 10^{-9} as compared to SNR = 20: 1) {2 × 2} phase-diversity receiver with delay demodulation, 2) dual-filter heterodyne demodulation, 3) optimum value of h.

TABLE I
THE NUMBER OF PHOTONS PER BIT IN ORDER TO ACHIEVE A BER OF 10^{-9} FOR VARIOUS CPFSK DEMODULATION METHODS

Receiver-Demodulation Method	Single Filter	Dual Filter	Delay
{2 × 2} phase diversity	76	44	20
{3 × 3} phase diversity	80	46.5	18.5
{2 × 2} phase & polar. diversity	82		22
{3 × 3} phase & polar. diversity	85		19.5
Ideal heterodyne	72	36	18

follows from the comparison that the delay demodulation is superior up to about $\delta_l T = 4\%$ which corresponds to about $h_{opt} = 3$, whereas the dual-filter method is better for greater values of this parameter. This is similar to the results of [3], where the boundary value of h is found to be 2 for the heterodyne detection without considering the noise correlation. As it should be expected h_{opt} increases when $\delta_l T$ increases.

VII. CONCLUSIONS

We have considered the BER performance of various CPFSK demodulation schemes. We have shown that for negligible laser linewidths the delay demodulation with $h = 0.5$ (i.e., MSK) outperforms the dual-filter scheme by roughly 6 dB as it comes to the signal level requirements. Of this 6 dB there stems 3 dB from the delay and multiply demodulation method and another 3 dB originates from the fact that for MSK the noise bandwidth is roughly twice as small as for the larger modulation indexes. The dual-filter method in its turn outperforms the single-filter method by another 3 dB. There is little sense however, in using the dual-filter method with phase-diversity receivers as then its main advantage, namely the baseband processing, is lost. But, nevertheless, it allows the receiver circuits to be designed for lower frequencies. When the laser linewidths increase, the performance of the dual detection scheme is approaching that of the delay demodulation and the former method is superior for $\delta_l T > 4\%$.

It is necessary to stress that CPFSK delay demodulation has the same performance as DPSK, but it is more flexible and can handle larger values of $\delta_l T$. The analysis presented may be easily adapted to treat DPSK systems.

APPENDIX A

For binary signaling, the spectrum with the frequency normalized to the bit rate is given by [17]

$$\Phi_u(f) = A_1^2(f) + A_2^2(f) + B_{11}(f)A_1^2(f) + 2B_{12}(f)A_1(f)A_2(f) + B_{22}(f)A_2^2(f) \quad \text{(A1)}$$

where

$$A_1(f) = \sin(\pi f + \pi h/2)/(\pi f + \pi h/2) \quad \text{(A2)}$$

$$A_2(f) = \sin(\pi f - \pi h/2)/(\pi f - \pi h/2) \quad \text{(A3)}$$

$$B_{11}(f) = [\cos(2\pi f + \pi h) - \cos^2(\pi h)]/D(f) \quad \text{(A4)}$$

$$B_{12}(f) = [\cos(2\pi f) - \cos(\pi h)]/D(f) \quad \text{(A5)}$$

$$B_{22}(f) = [\cos(2\pi f - \pi h) - \cos^2(\pi h)]/D(f) \quad \text{(A6)}$$

and

$$D(f) = 1 + \cos^2(\pi h) - 2\cos(\pi h)\cos(2\pi f) \quad \text{(A7)}$$

under the condition that h is not an integer number [17]. We have dropped in (A1) a constant multiplication factor as we are only interested in relative values. For a large modulation index $h \gg 1$, there is no overlap of the spectra related to "ZERO" and "ONE" frequencies (see (A2) and (A3)), that is the cross terms in (A1) are zero. To simplify the analysis let us assume that

$$h = 2k + \pi/2, \qquad k = 1, 2, \cdots \quad \text{(A8)}$$

which gives a compact spectrum near the (normalized to the bit rate) frequencies $\pm h/2$. After shifting the frequency to zero we get

$$\Phi_u(f) \sim [\sin(\pi f)/(\pi f)]^2[1 + \cos(2\pi f)]. \quad \text{(A9)}$$

APPENDIX B

Let us introduce the following random variables:

$$x_1 = 0.5[(n_1 - n_1')/\sqrt{1-\rho} + (n_0 + n_0')/\sqrt{1+\rho}]$$
$$x_2 = 0.5[(n_1 - n_1')/\sqrt{1-\rho} - (n_0 + n_0')/\sqrt{1+\rho}]$$
$$x_3 = 0.5[(n_1 + n_1')/\sqrt{1+\rho} + (n_0 - n_0')/\sqrt{1-\rho}]$$
$$x_4 = 0.5[(n_1 + n_1')/\sqrt{1+\rho} - (n_0 - n_0')/\sqrt{1-\rho}]$$
$$-1 < \rho < 1. \quad \text{(A10)}$$

They are Gaussian as they consist of sums of Gaussian variables. By examining their cross correlations, which are zero in each case, it is easy to prove that they are not correlated. Thus they are independent. Furthermore, they have unit variances. We have then

$$n_0 = 0.5[(x_1 - x_2)\sqrt{1+\rho} + (x_3 - x_4)\sqrt{1-\rho}]$$
$$n_0' = 0.5[(x_1 - x_2)\sqrt{1+\rho} - (x_3 - x_4)\sqrt{1-\rho}]$$
$$n_1 = 0.5[(x_1 + x_2)\sqrt{1-\rho} + (x_3 + x_4)\sqrt{1+\rho}]$$
$$n_1' = 0.5[-(x_1 + x_2)\sqrt{1-\rho} + (x_3 + x_4)\sqrt{1+\rho}]. \quad \text{(A11)}$$

Let us insert these values into (26) and multiply it by $2/\sqrt{(1-\rho^2)}$ which does not influence its sign. We have, after some algebraic manipulations

$$\begin{aligned} w' &= 2w/\sqrt{(1-\rho^2)} \\ &= (x_1+v_1)^2 + (x_4+v_4)^2 \\ &\quad - (x_2+v_2)^2 - (x_3+v_3)^2 \end{aligned} \tag{A12}$$

where

$$\begin{aligned} v_1 &= \frac{0.5A}{\sqrt{1-\rho^2}}[\sqrt{1-\rho}\sin(\alpha+\Delta) + \sqrt{1+\rho}\sin\alpha \\ &\quad + \sqrt{1+\rho}\cos(\alpha+\Delta) + \sqrt{1-\rho}\cos\alpha] \\ v_2 &= \frac{0.5A}{\sqrt{1-\rho^2}}[\sqrt{1-\rho}\sin(\alpha+\Delta) - \sqrt{1+\rho}\sin\alpha \\ &\quad - \sqrt{1+\rho}\cos(\alpha+\Delta) + \sqrt{1-\rho}\cos\alpha] \\ v_3 &= \frac{0.5A}{\sqrt{1-\rho^2}}[\sqrt{1+\rho}\sin(\alpha+\Delta) - \sqrt{1-\rho}\sin\alpha \\ &\quad + \sqrt{1-\rho}\cos(\alpha+\Delta) - \sqrt{1+\rho}\cos\alpha] \\ v_4 &= \frac{0.5A}{\sqrt{1-\rho^2}}[\sqrt{1+\rho}\sin(\alpha+\Delta) + \sqrt{1-\rho}\sin\alpha \\ &\quad - \sqrt{1-\rho}\cos(\alpha+\Delta) + \sqrt{1+\rho}\cos\alpha]. \end{aligned} \tag{A13}$$

Then the probability that $w < 0$ is equal to the probability that

$$\sqrt{(x_1+v_1)^2+(x_4+v_4)^2} < \sqrt{(x_2+v_2)^2+(x_3+v_3)^2}. \tag{A14}$$

The pdf of either side of the inequality above is generalized chi with $N = 2$ and the noncentral parameters

$$\begin{aligned} v_1^2 + v_4^2 &= A_\chi^2 \\ &= 2\text{SNR}\,[1 + \sqrt{1-\rho^2}\cos\Delta - \rho\sin\Delta]/(1-\rho^2) \\ v_2^2 + v_3^2 &= A_\chi^2 \\ &= 2\text{SNR}\,[2 - \sqrt{1-\rho^2}\cos\Delta - \rho\sin\Delta]/(1-\rho^2) \end{aligned} \tag{A15}$$

while the BER is given by (21) [9] with these pdf's inserted into it.

Appendix C

We shall neglect the noise correlation in this section and assume that all the noises are uncorrelated, i.e., $\langle n_k n_i\rangle = \langle n_k' n_i\rangle = \langle n_k' n_i'\rangle = 0$ for $k \neq i$. Let us introduce the following random variables

$$\begin{aligned} x_1 &= [(2n_0 - n_1 - n_2)/2 + (n_1' - n_2')/\sqrt{2}]/\sqrt{2} \\ x_2 &= [(2n_0 - n_1 - n_2)/2 - (n_1' - n_2')/\sqrt{2}]/\sqrt{2} \\ x_3 &= [(2n_0' - n_1' - n_2')/2 + (n_1 - n_2)/\sqrt{2}]/\sqrt{2} \\ x_4 &= [(2n_0' - n_1' - n_2')/2 - (n_1 - n_2)/\sqrt{2}]/\sqrt{2}. \end{aligned} \tag{A16}$$

They are Gaussian as they consist of sums of Gaussian variables. By examining their cross correlations, which are zero in each case, it is easy to prove that they are not correlated. Thus they are independent. Furthermore, they have unit variances. We have then

$$\begin{aligned} n_1' - n_2' &= x_1 - x_2 \\ n_1 - n_2 &= x_3 - x_4 \\ 2n_0 - n_1 - n_2 &= \sqrt{2}(x_1 + x_2) \\ 2n_0' - n_1' - n_2' &= \sqrt{2}(x_3 + x_4). \end{aligned} \tag{A17}$$

Substituting these into (47) and multiplying it by $3\sqrt{1.5}$, which does not influence its sign, we have after some algebraic manipulation

$$\begin{aligned} w' &= 3\sqrt{1.5}\,w \\ &= (x_2+v_2)^2 + (x_3+v_3)^2 \\ &\quad - (x_1+v_1)^2 - (x_4+v_4)^2 \end{aligned} \tag{A18}$$

where

$$\begin{aligned} v_1 &= (\sqrt{3}A/2)[\cos(\alpha+\Delta) - \sqrt{1.5}\cos\alpha] \\ v_2 &= (\sqrt{3}A/2)[\cos(\alpha+\Delta) + \sqrt{1.5}\cos\alpha] \\ v_3 &= -(\sqrt{3}A/2)[\sin(\alpha+\sqrt{1.5}\sin(\alpha+\Delta)] \\ v_4 &= (\sqrt{3}A/2)[-\sin\alpha + \sqrt{1.5}\sin(\alpha+\Delta)]. \end{aligned} \tag{A19}$$

Then the probability that $w < 0$ is equal to the probability that

$$\sqrt{(x_1+v_1)^2+(x_4+v_4)^2} > \sqrt{(x_2+v_2)^2+(x_3+v_3)^2}. \tag{A20}$$

The pdf of either side of the inequality above is generalized chi with $N = 2$ and the noncentral parameters

$$\begin{aligned} v_2^2 + v_3^2 &= A_\chi^2 \\ &= 2\text{SNR}\,\{1 + 0.25[\sin^2(\alpha+\Delta) + \cos^2\alpha] + \sqrt{1.5}\cos\Delta\} \\ v_1^2 + v_4^2 &= A_\xi^2 \\ &= 2\text{SNR}\,\{1 + 0.25[\sin^2(\alpha+\Delta) + \cos^2\alpha] - \sqrt{1.5}\cos\Delta\} \end{aligned} \tag{A21}$$

while the BER is given by (21) [9] with these pdf's inserted into it.

References

[1] K. Iwashita and T. Matsumoto, "Modulation and detection characteristics of optical continuous phase FSK transmission system," *J. Lightwave Technol.*, vol. LT-5, no. 4, pp. 452–460, Apr. 1987.

[2] J. L. Gimlett *et al.*, "A 2-Gbit/s optical FSK heterodyne transmission experiment using a 1520-nm DFB laser transmitter," *J. Lightwave Technol.*, vol. LT-5, no. 9, pp. 1315–1323, Sept. 1987.
[3] K. Emura *et al.*, "An optical FSK heterodyne dual-filter detection system for taking advantage of DFB LD applications," *J. Lightwave Technol.*, vol. 8, no. 2, pp. 243–250, Feb. 1990.
[4] I. Garrett and G. Jacobsen, "Theory for optical heterodyne narrow-deviation FSK receivers with delay demodulation," *J. Lightwave Technol.*, vol. 6, no. 9, pp. 1415–1423, Sept. 1988.
[5] G. Jacobsen *et al.*, "Bit error rate floors in coherent optical systems with delay demodulation," *Electron. Lett.*, vol. 25, no. 21, pp. 1425–1427, Oct. 1989.
[6] G. Jacobsen and L. G. Kazovsky, "CPFSK coherent optical receivers: Impact of IF bandwidth and laser phase noise," *Electron. Lett.*, vol. 24, no. 11, pp. 715–717, May 1988.
[7] L. Kazovsky and G. Jacobsen, "Bit error ratio of CPFSK coherent optical receivers," *Electron. Lett.*, vol. 24, no. 1, pp. 69–70, Jan. 1988.
[8] K. Emura *et al.*, "Optimum system design for CPFSK heterodyne delay demodulation systems with DFB LD's," *J. Lightwave Technol.*, vol. 8, no. 2, pp. 251–258, Feb. 1990.
[9] J. Siuzdak and W. van Etten, "BER evaluation for phase and polarization diversity optical homodyne receivers using noncoherent ASK and DPSK demodulation," *J. Lightwave Technol.*, vol. 7, no. 4, pp. 584–599, Apr. 1989.
[10] J. Siuzdak and W. van Etten, "Heterodyne ASK multiport optical receivers using postdetection filtering," *J. Lightwave Technol.*, vol. 8, no. 1, pp. 71–77, Jan. 1990.
[11] Y.-H. Cheng, T. Okoshi, and O. Ishida, "Performance analysis and experiment of a homodyne receiver insensitive to both polarization and phase fluctuations," *J. Lightwave Technol.*, vol. 7, no. 2, pp. 368–374, Feb. 1989.
[12] L. Kazovsky, P. Meissner, and E. Patzak, "ASK multiport optical homodyne receivers," *J. Lightwave Technol.*, vol. LT-5, pp. 770–790, 1987.
[13] R. Noe *et al.*, "New FSK phase diversity receiver in a 150 Mbit/s coherent optical transmission system," *Electron. Lett.*, vol. 24, no. 9, pp. 567–568, Apr. 1988.
[14] W. R. Leeb, "Realization of 90 and 180 degree hybrids for optical frequencies," *Archiv für Electronik und Übertragungstechnik*, vol. 37, pp. 203–206, 1983.
[15] L. G. Kazovsky *et al.*, "All-fiber 90° optical hybrid for coherent communications," *Appl. Opt.*, vol. 26, pp. 437–439, 1987.
[16] A. W. Davis *et al.*, "Phase diversity techniques for coherent optical receivers," *J. Lightwave Technol.*, vol. LT-5, pp. 561–572, 1987.
[17] J. G. Proakis, *Digital Communications*. New York: McGraw-Hill, 1983.
[18] G. Nicholson, "Probability of error for optical heterodyne DPSK systems with quantum phase noise," *Electron. Lett.*, vol. 20, no. 24, pp. 1005–1007, Nov. 1984.
[19] W. van Etten and J. van der Plaats, *Fundamentals of Optical Fiber Communications*. London: Prentice-Hall, 1991.
[20] R. Noe, "Sensitivity comparison of coherent optical heterodyne, phase diversity, and polarization diversity receivers," *J. Opt. Commun.*, vol. 10, no. 1, pp. 11–18, 1989.
[21] H. W. Tsao, J. Wu, and Y. H. Lee, "Performance analysis of optical phase diversity FSK receiver using delay-and-multiplying discriminator," *J. Opt. Commun.*, vol. 10, no. 3, pp. 97–100, 1989.

*

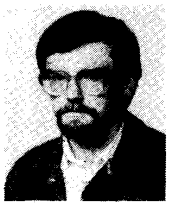

Jerzy Siuzdak was born in 1955 in Kraków, Poland. He graduated from Warsaw University of Technology where he obtained the M.S. and Ph.D. degrees in 1979 and 1982, respectively.

Starting in 1982 he was employed by the Institute of Telecommunications, Warsaw, where he worked on optoelectronic and range measuring equipment. His interests include phase measurement, signal estimation, and some aspects of light propagation. In 1987, he began work at the Technical University of Eindhoven, Eindhoven, The Netherlands, on leave from Poland. He is involved in research on coherent optical communication systems.

*

W. van Etten (M'80–SM'91) was born in Zevenbergen, The Netherlands, in 1942. He received the M.Sc. and Ph.D. degrees in electrical engineering from Eindhoven University of Technology, Eindhoven, The Netherlands, in 1969 and 1976, respectively.

From 1969 to 1970 he was employed by Philips Gloeilampenfabrieken, developing circuits for oscilloscopes. In 1970 he was appointed an Assistant Professor at Eindhoven University of Technology, Department of Electrical Engineering. From 1970 to 1976 he was engaged in research on the transmission of digital signals via coaxial and multiwire cables. Since 1976 he has been involved with research and education on optical fiber communications. Presently, he is an Associate Professor at the Eindhoven University of Technology.